Advances in Computational Sciences and Technology
ISSN 0973-6107 Volume 11, Number 1 (2018) pp. 1-13

http://www.ripublication.com

Automatic Optic Disc Localization in Color Retinal Fundus Images

Thresiamma Devasia
Dept. of Computer Science, Assumption College Changanacherry, Kerala, India.

Poulose Jacob
Dept. of Computer Science, Cochin University of Science and Technology Cochin, India.

Tessamma Thomas
Dept. of Electronics, Cochin University of Science and Technology Cochin, India.

Abstract

The optic disc in a healthy retinal image usually appears as a bright yellowish and circular shaped object which is partly covered with blood vessels. Diseases with symptoms on the fundus images are very complex. For the optic disc, differences in the color, shape, edge or vasculature may signify a pathological change. The information about the optic disc can be used to detect the severity of some diseases such as glaucoma. Optic disc localization is an important step in automatic diagnosis of various serious ophthalmic pathologies. Optic disc localization is a difficult task due to the variations in optic disc shape, size, and color pointed out, there are some additional complications to take into account. The most difficult problem of optic disc extraction is to locate the region of interest. More over it is a time consuming task. In this paper a new method is used for the automatic optic disc localization. This methodology uses morphological operations and edge detection techniques followed by the Circular Hough Transform to localize the optic disc. The technique is tested on 549 images from publicly available DRIVE, DRION, HRF, DIARETDB0 and DIARETDB1 databases and, Live images from hospitals. The new method achieves an average success rate of 97.27 percentage for the localization of optic disk. The accuracy is obtained by comparing the accuracy of the obtained centroid against the hand labeled ground truth produced by a clinician. The expert traced centroid is used as the ground truth to facilitate the performance analysis using the comparison of

ground truth center with the obtained center of the OD. The scatter plot analysis gives a high positive correlation between the ground truth centroids and obtained centroids. This computerized detection of optic disc is very useful for the automatic screening of retinal diseases.

INTRODUCTION

Fundus imaging is a common clinical procedure used to record a viewing of the retina. In a color retinal image the optic disc is the brightest region in the retinal image and the blood vessels originate from its center. The central portion of disc is the brightest region called optic cup, where the blood vessels and nerve fibers are absent. [1] Fig.1 shows the main features such as optic disc, optic cup and blood vessels of a color retinal image.

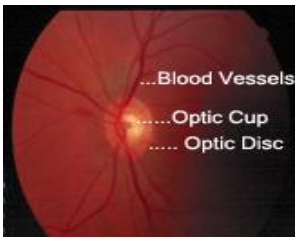

Figure 1. Color fundus image

Optic disc (OD) is a key reference for automatic screening of retinal diseases. In ophthalmology, the automatic detection of OD may be of considerable interest for computer assisted diagnosis. Detecting OD in the human retina like is a time consuming task for ophthalmologists and prone to human error. That is why much effort has been done to detect OD in the human retina automatically.

The detection of the optic disc is the first step in the early detection of certain retinal diseases. The location of OD is of critical importance in retinal image analysis. This research paper carries out a new automated methodology to detect the OD in retinal images. OD detection helps the ophthalmologists to find whether the patient is affected by retinal diseases or not. The new technique is to use edge detection and Circular Hough transform which gives higher percentage of detection than the already existing methods. The purpose of this study is to automatically detect the position of the OD in digital retinal fundus images.

RELATED WORK

In a color retinal image the optic disc belongs to the brighter parts along with some lesions. The central portion of disc is the brightest region called optic cup, where the blood vessels and nerve fibers are absent. Different OD location methods reported in the literature. H Li et al. [2] proposed a new method to localize optic disc center. The candidate regions were first determined by clustering the brightest pixels in retinal images. Principal component analysis was applied to these candidate regions. R. A.

Abdel-Ghafar et al. [3] developed automated techniques of generating quantitative descriptions of the retinal images that might be used in diagnosis and assessment. Carmona et al. [4] used genetic algorithm method to obtain an ellipse approximating the optic disc in retinal images. Youssif et al. [5] used directional pattern of the retinal blood vessels to localize the center of optic disc. Rangayyan et al. [6] proposed a method for OD detection. In this method, optic disc center was localized based on the property that it appears as the focal point of the blood vessels in retina mage. D Welfer et al. [7] developed a method for OD detection using an adaptive morphological approach. A. Aquino et al. [8] developed a method to locate OD using the initial information of OD. For this purpose, a location methodology based on a voting-type algorithm is also proposed. Muramatsu et al. [9] developed an algorithm based on pixel classification. In this method every pixel in the retina image will be classified into a class, such as optic disc or background pixel. Cemal Köse et al. [10] used statistical techniques for the detection of the optic disc. Amin Dehghani et al.[11] proposed a method for localizing the center of optic disc using the average of histograms for each color component. Saleh Shabbier et al. [12] developed a method using the principle-component-analysis-based preprocessing and curvelet transform for optic disc extraction.

In this paper, Canny edge detection and Circular Hough transforms are applied on the *I* component of the *HSI* model for OD localization.

The rest of the paper is organized as follows. Section III describes the materials used for the new method. In Section IV the developed algorithm is given. The results are presented in Section V, and conclusions are given in Section VI.

MATERIALS AND METHODS

The images used in this paper are obtained from four public databases DRIVE, DRION, DIARETDB0 and DIARETDB1, and the images obtained from Giridhar Eye Research Institute Kochi. A total of 549 images including, 86 normal images and 463 diseased images and are used in this paper for evaluation. The images are of very large variability in terms of disc size and image quality.

THE NEW ALGORITHM

This section presents the new OD detection technique. In particular, this section is divided into three subsections, which deal with the retinal image pre-processing, OD detection, and discussion respectively.

Retinal Image Pre-processing

Retinal images need to be pre-processed before the OD detection. As the new technique makes use of the circular brightness structure of the OD, the HSI color space of the color retinal fundus image is first extracted.

Conversion from RGB to HSI

The *HSI* colour space (hue, saturation and intensity) attempts to produce a more intuitive representation of colour. The *H* and *S* axes are polar coordinates on the plane orthogonal to *I*. *Hue* thus represent what humans implicitly understand as colour. *S* is the magnitude of the colour vector projected in the plane orthogonal to *I*, and so represents the difference between pastel colours (low saturation) and vibrant colours (high saturation). The *I* axis represents the luminance information. The *HSI* model is also a more useful model for evaluating or measuring an object's color characteristics, such as the redness or the yellowness of an image. So the *HSI* model is used in this paper for the OD localization. First of all the range of the R, G, and B components are normalized to the interval from 0 to 1. Then the values r, g, b are computed using the following formulae.

$$r = R/(R + G + B) \quad (1)$$

$$g = G/(R + G + B) \quad (2)$$

$$b = B/(R + G + B) \quad (3)$$

When the RGB cube is considered, then all possible triples (r, g, b) lie on a triangle with corners (1, 0, 0), (0, 1, 0), and (0, 0, 1).

The intensity is given by

$$I = \frac{r + g + b}{3} \quad (4)$$

where the quantities r, g and b are the amounts of the red, green and blue components, normalized to the range [0,1]. The intensity is therefore just the average of the red, green and blue components. The saturation is given by:

$$S = 1 - 3/(r + g + b)[\min(r, g, b)] \quad (5)$$

where the min(r, g, b) term is really just indicating the amount of white present. If any of r, g or b are zero, there is no white and we have a pure colour.

$$H = \cos^{-1}[(r - \tfrac{1}{2}g - \tfrac{1}{2}b)/\sqrt{r^2 + g^2 + b^2 - rg - rb - rb}] \text{ if } g \geq b,$$

or

$$H = 360 - \cos^{-1}[(r - \tfrac{1}{2}g - \tfrac{1}{2}b)/\sqrt{r^2 + gb + b^2 - rg - rb - gb}]$$

$$\text{if } b > g, \quad (6)$$

where the inverse cosine output is in degrees.

Intensity *I* is overall lightness or brightness of the color, defined numerically as the average of the equivalent r, g, b values [13]. In this paper the *I* component within the HSI color space is used, for the OD detection, since OD is the brightest part of the fundus image.

Blood Vessel Removal

The blood vessels within the OD are distracters for the OD extraction. In this method a morphological closing operation is performed on the *I* component. The dilation operation first removes the blood vessels and then the erosion operation approximately restores the boundaries to their former position. The closing operation is given in the following equation.

Closing : $C(A,B) = A \bullet B = E(D(A,-B),-B)$, (7)

where A is the *I* component HSI image of the input image and B is a 10x10 symmetrical disc structuring element, to remove the blood vessels[14]. C is the resultant vessel free, smoothed output image.

Figure 2 shows the preprocessing operation corresponding to the input image.

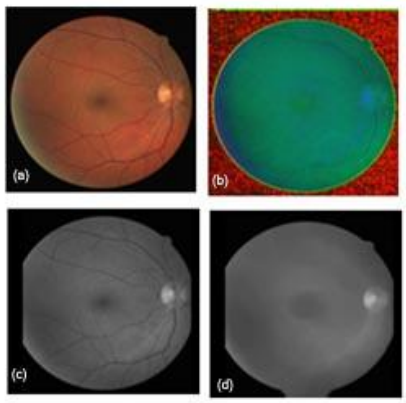

Figure 2. Preprocessing steps (a) Input image
(b) HSI image (c) I component
(d) Vessel free I component

Edge Detection

The equations are an exception to the prescribed specifications of this template. You will need to determine whether or not your equation should be typed using either the Times New Roman or the Symbol font (please no other font). To create multileveled equations, it may be necessary to treat the equation as a graphic and insert it into the text after your paper is styled.

Edges characterize boundaries in image processing. An edge point is the location in which there is a strong intensity contrast, ie. the transition between a pure white and a pure black region. At such a point, there are consecutive 1s in one direction and consecutive 0s in the other direction. To determine the edge points, the image was scanned line by line in a direction.

The Canny Edge Detection Algorithm

Mainly three criteria are used in canny edge detector. The first and most obvious is low error rate. The second criterion is that the edge points be well localized. In other words, the distance between the edge pixels as found by the detector and the actual edge is to be at a minimum. A third criterion is to have only one response to a single edge. This was implemented because the first 2 were not substantial enough to completely eliminate the possibility of multiple responses to an edge.

Based on these criteria, the algorithm runs in 5 separate steps. The algorithm steps are given below.

Step1. Smoothing: Blurring of the image to remove noise.

Let f(x, y) denote the input image and G(x, y) denote the Gaussian function:

$$G(x, y) = e^{-(x^2 + y^2/2 a^2)} \quad (8)$$

A smoothed image $f_s(x, y)$ is formed by convolving G and f:

$$f_s(x, y) = G(x, y) * f(x, y) \quad (9)$$

Step2. Finding gradients: The edges should be marked where the gradients of the image has large magnitudes.

Compute the gradient, magnitude and direction (angle):

$$gx = \partial fs/\partial x \quad (10)$$

$$gy = \partial f_s/\partial y \quad (11)$$

$$M(x, y) = \sqrt{gx^2 + gy^2} \quad (12)$$

$$a(x, y) = \arctan(gy/gx), \quad (13)$$

Step3. Non-maximum suppression: Only local maxima should be marked as edges.

The gradient M(x, y) typically contains wide range around local maxima. Next step is to thin those ridges.

Nonmaxima Suppression:

Let d_1, d_2, d_3, and d_4 denote the four basic edge directions for a 3×3 region: horizontal, -45 degrees, vertical, +45 degrees, respectively.

1. Find the direction d_k that is closest to a(x,y)
2. If the value of M(x, y) is less than at least one of its two neighbours along d_k,

Let gn(x, y) = 0(suppression); otherwise, let gn(x,y) = M(x,y)

Step4. Double thresholding: Potential edges are determined by thresholding.

Final operation is to threshold gn(x, y) to reduce false edge points.

Step5. Edge tracking by hysteresis: Final edges are determined by suppressing all edges that are not connected to a very certain (strong) edge.

Hysteresis Thresholding:

Mathematically it is done like this:

gnh(x, y) = gn(x, y) >= Th

gnl(x,y) = gn(x,y) >= Tl

and

gnl(x, y) = gnl(x, y) – gnh(x, y)

Depending on the value of *Th*, the edges in gnh(x, y) typically have gaps. Longer edges are formed using the following procedure:

(a) Locate the next unvisited edge pixel p, in gnh(x, y)

(b) Mark as valid edge pixel all the weak pixels in gnl(x, y) that are connected to p using 8-connectivity.

(c) If all non-zero pixel in gnh(x, y) that were not marked as valid edge pixels. [13]

The *canny* function from the tool box is used for getting the edge image [14]. The edge image and image after removing the unwanted objects are in figures Figure 3(a) and 3(b).

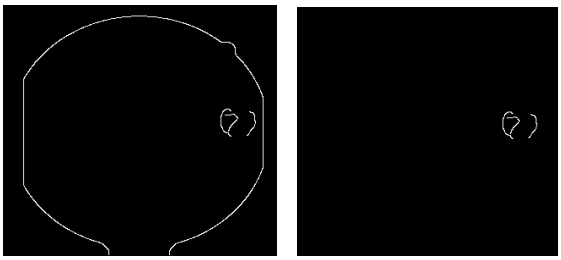

Figure 3(a) Edge Image after canny edge detection
(b) Image after removing unwanted objects

Hough transform

After the edge detection has been completed, the Hough transform was applied to get the optic nerve disc localization, because the optic disc structure in retinal images is nearly circular. In the case of a circle, there are three parameters: two parameters indicate the centre of the circle and one parameter the radius. In this scheme the parameter space is congruent with the image space, that is, each point in the image maps to a point in the same position in the parameter space. To detect a circle of radius *r*, the circles of this radius are plotted in the Hough parameter space centered on every edge pixel found in the image. Thus, an array of peaks is formed for each edge detected fundus image. A peak emerges when the circles in the Hough space

intersect one another. Such peaks in the Hough parameter space indicate the possible centers of *r* radius circles. The problem is that the user does not know both: where the OD lies in the retinal image and how large it is. Therefore, the circular Hough transform is iterated at each time with the different circle radius *r* and selects the highest peak value in the peak array formed.

After the parameters for the circle have been selected, the approximate OD centre is found and the Circle detection is done using Hough transform.

The following steps are used to find the radius and center of OD from the smoothed image.

1. Doing Edge detection on the image - The Canny edge detector with 0.1 and 0.2 as the low and high thresholds is used in this paper. This removed most of the noise due to the texture leaving only the edges of the within the smoothed image.
2. Hough Transform computation - Firstly the radius of the OD is computed based on the highest size of the edge in the edge image obtained after removing the unwanted objects.

   The radii obtained are 47, 30, 27 and 19. The function hough circle computes the transform [14]. For each edge pixel, it first runs through a sequence of x-values and computes the corresponding y-values for that radius. It then runs through a sequence of y-values and computes the corresponding x-values for that radius. The sequence of x-values varies from

   x(edge-pixel) - (radius/cos(45)) to

   x(edge-pixel) + (radius/cos(45)) [13].

   The same is true for the sequence of y-values. The two sequences are so processed because as the points reach the x (y)-axis, the same y(x)-value for different x(y)-values is got , for points lying on the circle corresponding to the hough transform. This choice of sequences does not let any bias to be introduced because of choice of an x or a y sequence.
3. Detecting Center - Once the *hough* transform image for a particular radius is computed, it is adjusted to lie between 0 and 1 and thresholded, so as to leave only those points with high probability of being the centers. The resulting point-set is then labeled with the OD region. The centroid of this region is considered as center of the detected OD.

Optic Disc Localization

The output image is obtained by locating the above mentioned centroid and radius as the center and radius of the input image. Fig. 4 (a) shows the edge image after applying circular hough transform and Fig. 4 (b) depicts the OD localization using the blue cross on the input image.

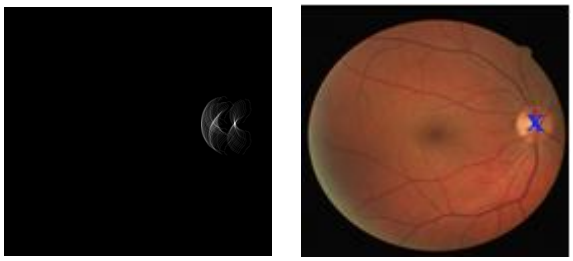

(a) **(b)**

Figure 4 (a) Image after applying circular Hough transform
(b) Optic Disc Localization using the blue cross

RESULTS AND DISCUSSIONS

The new algorithm was applied on publicly available fundus photographs and the optic disc was detected. The validation of the method has been carried out on four public databases DRIVE, DRION, HRF, DIARETDB0 and DIARETDB1 databases and images from two ophthalmologists. The obtained results and performance analysis are explained in this section.

The performance analysis was done using the ground truth optic disc diameters of HRF database and manually marked borders of the OD for other databases. The details are explained in the following section.

Image Data Set

The template is designed so that author affiliations are not repeated each time for multiple authors of the same affiliation. Please keep your affiliations as succinct as possible (for example, do not differentiate among departments of the same organization). This template was designed for three affiliations.

1) **The HRF database**

The HRF database has been newly established during the cooperation with Pattern Recognition Lab at the University of Erlangen–Nuremberg, Germany and Tomas Kubena's Ophthalmology Clinic, Zlin, Czech Republic, where images were acquired. The goal of this dataset is to support comparative studies on automatic segmentation algorithms on retinal images. The database can be downloaded from public websites. The database contains three sets of fundus images: of healthy, glaucomatous, and diabetic retinopathy subjects (15 images in each group). The images were acquired with CANON CF-60 UVi camera equipped with CANON EOS-20D with a 60-degree FOV. The image size is 3504 × 2336 pixels. All images are 24-bits per pixel and are stored in JPEG format.

2) **The DIARETDB0 and DIARETDB1 Databases**

The DIARETDB0 and DIARETDB1 Database images were captured using an FOV of 50° and the size of each image is 1500 x 1152 x 3. Out of the 130 images of the DIARETDB0 database, 20 have normal architecture and 110 have various types of pathology. Out of the 89 images of the DIARETDB1 database, 5 have normal architecture and 84 have various types of pathology.

3) **DRION Database**

It has 110 retinal images with each image having the resolution of 600 x 400 pixels and the optic disc annotated by two experts with 36 landmarks. The mean age of the patients was 53.0 years (standard Deviation 13.05), with 46.2% male and 53.8% female and all of them were Caucasian ethnicity 23.1% patients had chronic simple glaucoma and 76.9% eye hypertension. The images were acquired with a colour analogical fundus camera, approximately centered on the ONH and they were stored in slide format. In order to have the images in digital format, they were digitized using a HP-PhotoSmart-S20 high-resolution scanner, RGB format, resolution 600x400 and 8 bits/pixel. Independent contours from 2 medical experts were collected by using a software tool provided for image annotation. In each image, each expert traced the contour by selecting the most significant papillary contour points and the annotation tool connected automatically adjacent points by a curve.

4) **DRIVE Database**

The images were acquired using a Canon CR5 non-mydriatic 3CCD camera with a 45 degree field of view (FOV). Each image was captured using 8 bits per color plane at 768 by 584 pixels. The set of 40 images has been divided into a training and a test set, both containing 20 images.

5) **Images from ophthalmologists**

75 images from Giridhar Eye Institute, Kochi was also used in this paper. All the images were obtained using Carlzeiss fundus camera. In total 5 are normal images and remaining 70 are diseased and the size of each image is 576 x 768 x 3. 65 images from Vassan Eye Clinic Kottayam was also used for the OD localization.

Implementation

The algorithm was applied on 549 images obtained from the above mentioned databases and ophthalmologists. Four of the input image from each data set, along with their OD localization on the input image, is shown in fig.5 (a) and fig.5 (b) respectively.

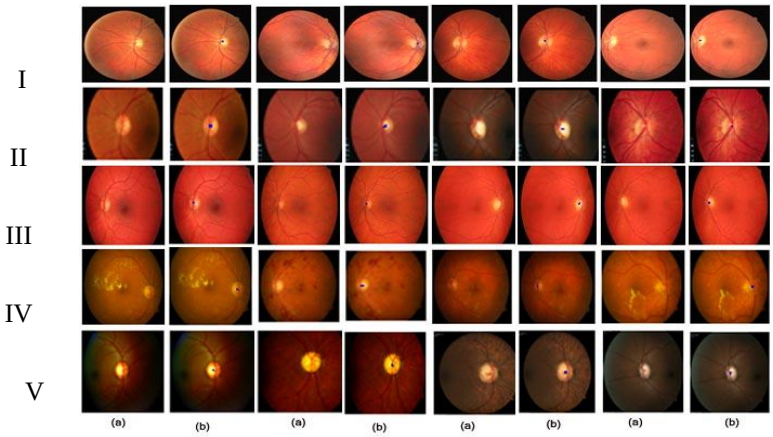

Figure 5 (a) Input Image **(b)** Localization of Optic Disc
I – DRIVE Database, II – DRION Database, III – HRF Database,
IV- DIARETDB0 and DIARETDB1Databases,
V – Images from Ophthalmologists I&II

The decision for successful localization or failed localization is based on human eye observation. Table 1 shows the success rate of the present method using DRIVE, HRF, DRION, DIARETDB0, DIARETDB1 databases and ophthalmologists.

Performance Analysis

a) Success Rate

Table 1. Optic Disc Localization result of present method

Database	***Total Images***	***Successful Detection***	***Successful Detection (%)***	***Time (secs.)***
DRIVE	40	38	95	0.43377
HRF	45	42	93.33	0.49927
DRION	110	110	100.00	0.56667
DIARETDB0	130	126	96.92	0.51568
DIARETDB1	89	86	96.63	0.59786
Ophthalmologist I	70	68	97.14	0.55088
Ophthalmologist II	65	64	98.46	0.59320
Total	549	534	97.27 (Average)	0.53676

b) Scatter plot Analysis

The accuracy is obtained by comparing the accuracy of the obtained centroid against the hand labeled ground truth produced by a clinician. The expert traced centroid is used as the ground truth to facilitate the performance analysis using the comparison of ground truth center with the obtained center of the OD. The statistical analysis is done using the scatter plot diagram. The ground truth x- coordinate (X1) and the ground

truth y-coordinate (Y1) are compared with and the obtained x-coordinate (X2) and, the obtained y-coordinate (Y2) of the centroids are plotted using the scatter plot diagram in Fig. 6. Fig. 6(a) shows the the scatter plot of X-coordinates and Fig. 6(b) shows the the scatter plot of Y-coordinates. From the scatter plot it is clear that there exists a highly positive linear relationship between both centroids.

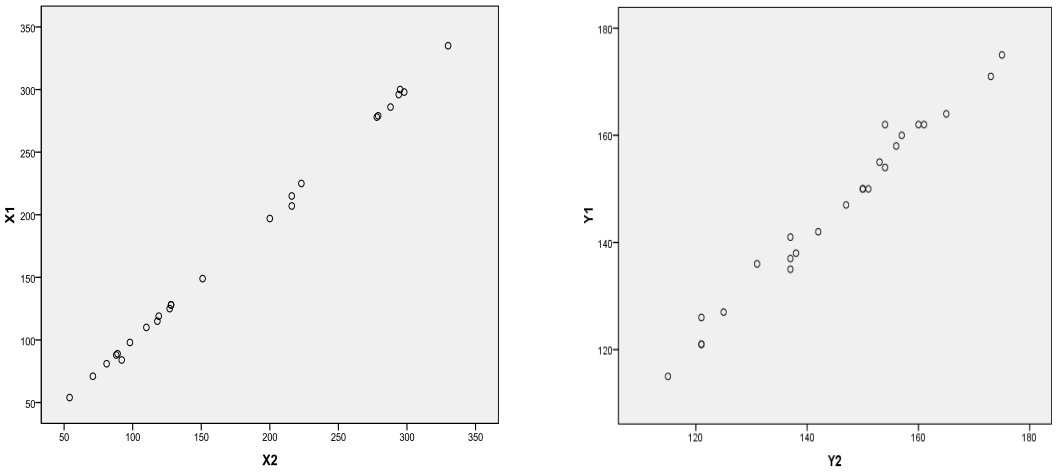

(a) (b)

Figure 6. Scatter plot diagram of (a) X-coordinates of ground truth and obtained centroid (b) Y-coordinates of ground truth and obtained centroid

CONCLUSION AND FUTURE WORK

In this study a new method to localise optic disc in retinal images is developed. The method is tested on 549 images from five publicly available databases and Live images from hospitals. The new method achieves an average accuracy of 97.3percentage for the localization of optic disk. This technique works pretty well even though the input image is in a low contrast condition. The main benefit of this work is the ability of the algorithm to reduce the processing time and improve processing consistency for each patient's fundus image, leading hopefully to an increase in efficiency and a reduction of cost.

REFERENCES

[1] M.B. Merickel, X. Wu, M. Sonka, M. Abramoff," Optimal images", Proc. SPIE Med. Imaging 6243 (2006), pp. 61433B-1-2.

[2] H. Li, O. Chutatape, "Automated feature extraction in color retinal images by a model based approach", IEEE Trans. Biomed. Eng. 51 () pp. 246–254., 2004

[3] R. A. Abdel-Ghafar & T. Morris, "Progress towards automated detection and characterization of the optic disc in glaucoma and diabetic retinopathy",

Medical Informatics and the Internet in Medicine, March; 32(1), pp. 19 – 25, 2007

[4] EJ Carmona, M Rincón, J García-Feijoo, JM Martínez-de-la-Casa, "Identification of the optic nerve head with genetic algorithms", Artif. Intell.Med. 43(3), pp. 243–259, PubMed Abstract | Publisher Full Text ,2008

[5] AA Youssif, AZ Ghalwash, AS Ghoneim, " Optic disc detection from normalized digital fundus images by means of a vessels' direction matched filter", IEEE Trans. Med. Imag. 27, pp. 11–18 , 2008

[6] RM Rangayyan, X Zhu, FJ Ayres, AL Ells, "Detection of the optic nerve head in fundus images of the retina with Gabor filters and phase portrait analysis", J. Digit. Imag. 23(4), pp. 438–453 (2010). Publisher Full Text

[7] D Welfer, J Scharcanski, CM Kitamura, MM Dal Pizzol, LWB Ludwig, DR Marinho, "Segmentation of the optic disk in color eye fundus images using an adaptive morphological approach", Comput. Biol. Med 40, pp. 124–137 (2010). PubMed Abstract | Publisher Full Text

[8] A. Aquino, M.E. Gegundez-Arias, D. Marin. "Detecting the optic disc boundary in digital fundus images using morphological, edge detection, and feature extraction techniques", IEEE Transactions on

[9] Medical Imaging, Nov., Volume 29, Issue 11, pp.1860–1869, 2010.

[10] Muramatsu, C., Nakagawa, T., Sawada, A., Hatanaka, Y Hara, T., Yamamoto, T., and Fujita, H., "Automated segmentation of optic disc region on retinal fundus photographs: Comparison of contour Modeling and pixel classification methods", Computer methods and programs in biomedicine, 101(1):23–32, 2011.

[11] Cemal Köse, Cevat İkibaş, "Statistical Techniques for Detection of Optic Disc and Macula and Parameters Measurement in Retinal Fundus Images", Journal of Medical and Biological Engineering, Vol. 31 No. 6, pp. 395-404, 2011

[12] AminDehghani, HamidAbrishami Moghaddam, Mohammad-Shahram Moin, "Optic disc localization in retinal images using histogram matching", EURASIP Journal on Image and Video Processing October 2012, pp. 2012-19, Date: 08 Oct 2012

[13] Journal of Optical Society of A merica, Vol. 30, Issue 1, pp. 13-21,2013.

[14] Rafael C Gonzalez, Richard E Woods, Steven L Eddins, Digital Image Processing, Prentice Hall Publications,2009

[15] Rafael C Gonzalez, Richard E Woods, Steven L Eddins., Digital Image Processing Using Matlab, Prentice Hall Publications,2009